

## 22.

# SEISMIC ANALYSIS USING DISPLACEMENT LOADING

*Direct use of Earthquake Ground Displacement in a  
Dynamic Analysis has Inherent Numerical Errors*

### 22.1 INTRODUCTION

{ XE "Displacement Seismic Loading" }Most seismic structural analyses are based on the relative-displacements formulation where the base accelerations are used as the basic loading. Hence, experience with the direct use of absolute earthquake displacement loading acting at the base of the structure has been limited. Several new types of numerical errors associated with the use of absolute seismic displacement loading are identified. Those errors are inherent in all methods of dynamic analysis and are directly associated with the application of displacement loading.

{ XE "Multi-Support Earthquake Motions" }It is possible for the majority of seismic analyses of structures to use the ground accelerations as the basic input, and the structural displacements produced are relative to the absolute ground displacements. In the case of multi-support input motions, it is necessary to formulate the problem in terms of the absolute ground motions at the different supports. However, the earthquake engineering profession has not established analysis guidelines to minimize the errors associated with that type of analysis. In this chapter, it will be shown that several new types of numerical errors can be easily introduced if absolute displacements are used as the basic loading.

{ XE "Bridge Analysis" } A typical long-span bridge structure is shown in Figure 22.1. Different motions may exist at piers because of local site conditions or the time delay in the horizontal propagation of the earthquake motions in the rock. Therefore, several hundred different displacement records may be necessary to define the basic loading on the structure.

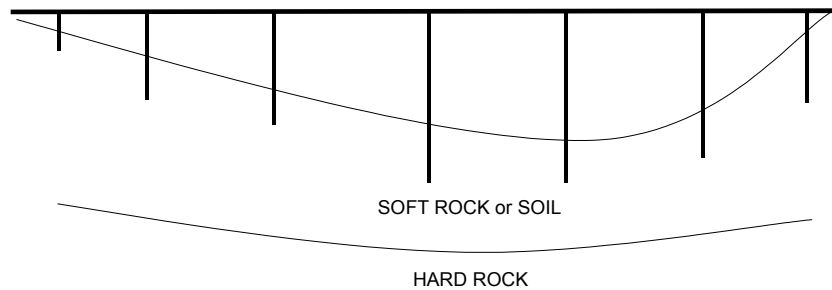


**Figure 22.1 Long Bridge Structure With Multi-Support Input Displacements**

The engineer/analyst must be aware that displacement loading is significantly different from acceleration loading with respect to the following possible errors:

1. The accelerations are linear functions within a time increment and an exact solution is normally used to solve the equilibrium equations. On the other hand, displacements derived from a linear acceleration function are a cubic function within each increment; therefore, a smaller time increment is required, or a higher order solution method must be used.
2. { XE "Relative Displacements" } The spatial distribution of the loads in the relative displacement formulation is directly proportional to the mass; and the 90 percent modal mass-participation rule can be used to ensure that the results are accurate. In the case of base displacement input, however, the modal mass-participation factors cannot be used to estimate possible errors. For absolute displacement loading, concentrated forces are applied at the joints near the fixed base of the structure; therefore, a large number of high-frequency modes are excited. Hence, alternative error estimations must be introduced and a very large number of modes may be required.

3. If the same damping is used for acceleration and displacement analyses, different results are obtained. This is because, for the same damping ratio, the effective damping associated with the higher frequency response is larger when displacement input is specified (see Table 19.1). Also, if mass proportional damping is used, additional damping is introduced because of the rigid body motion of the structure.

The dynamic equilibrium equations for absolute seismic displacement type of loading are derived. The different types of errors that are commonly introduced are illustrated by an analysis of a simple shear-wall structure.

## 22.2 EQUILIBRIUM EQUATIONS FOR DISPLACEMENT INPUT

For a lumped-mass system, the dynamic equilibrium equations in terms of the unknown joint displacements  $\mathbf{u}_s$  within the superstructure and the specified absolute displacements  $\mathbf{u}_b$  at the base joints can be written as:

$$\begin{bmatrix} \mathbf{M}_{ss} & \mathbf{0} \\ \mathbf{0} & \mathbf{M}_{bb} \end{bmatrix} \begin{bmatrix} \ddot{\mathbf{u}}_s \\ \ddot{\mathbf{u}}_b \end{bmatrix} + \begin{bmatrix} \mathbf{C}_{ss} & \mathbf{C}_{sb} \\ \mathbf{C}_{bs} & \mathbf{C}_{bb} \end{bmatrix} \begin{bmatrix} \dot{\mathbf{u}}_s \\ \dot{\mathbf{u}}_b \end{bmatrix} + \begin{bmatrix} \mathbf{K}_{ss} & \mathbf{K}_{sb} \\ \mathbf{K}_{bs} & \mathbf{K}_{bb} \end{bmatrix} \begin{bmatrix} \mathbf{u}_s \\ \mathbf{u}_b \end{bmatrix} = \begin{bmatrix} \mathbf{0} \\ \mathbf{R}_b \end{bmatrix} \quad (22.1)$$

The mass, damping and stiffness matrices associated with those displacements are specified by  $\mathbf{M}_{ij}$ ,  $\mathbf{C}_{ij}$ , and  $\mathbf{K}_{ij}$ . Note that the forces  $\mathbf{R}_b$  associated with the specified displacements are unknown and can be calculated after  $\mathbf{u}_s$  has been evaluated.

Therefore, from Equation (22.1) the equilibrium equations for the superstructure only, with specified absolute displacements at the base joints, can be written as:

$$\mathbf{M}_{ss} \ddot{\mathbf{u}}_s + \mathbf{C}_{ss} \dot{\mathbf{u}}_s + \mathbf{K}_{ss} \mathbf{u}_s = -\mathbf{K}_{sb} \mathbf{u}_b - \mathbf{C}_{sb} \dot{\mathbf{u}}_b \quad (22.2)$$

The damping loads  $\mathbf{C}_{sb} \dot{\mathbf{u}}_b$  can be numerically evaluated if the damping matrix is specified. However, the damping matrix is normally not defined. Therefore, those damping forces are normally neglected and the absolute equilibrium equations are written in the following form:

$$\mathbf{M}_{ss} \ddot{\mathbf{u}}_s + \mathbf{C}_{ss} \dot{\mathbf{u}}_s + \mathbf{K}_{ss} \mathbf{u}_s = -\mathbf{K}_{sb} \mathbf{u}_b = \sum_{j=1}^J \mathbf{f}_j u_j(t) \quad (22.3)$$

Each independent displacement record  $u_j(t)$  is associated with the space function  $\mathbf{f}_j$  that is the negative value of the  $j$ th column in the stiffness matrix  $\mathbf{K}_{sb}$ . The total number of displacement records is  $J$ , each associated with a specific displacement degree of freedom.

{ XE "Cubic Displacement Functions" } For the special case of a rigid-base structure, a group of joints at the base are subjected to the following three components of displacements, velocities and accelerations.

$$\mathbf{u}_b = \begin{bmatrix} u_x(t) \\ u_y(t) \\ u_z(t) \end{bmatrix}, \quad \dot{\mathbf{u}}_b = \begin{bmatrix} \dot{u}_x(t) \\ \dot{u}_y(t) \\ \dot{u}_z(t) \end{bmatrix}, \quad \text{and} \quad \ddot{\mathbf{u}}_b = \begin{bmatrix} \ddot{u}_x(t) \\ \ddot{u}_y(t) \\ \ddot{u}_z(t) \end{bmatrix} \quad (22.4)$$

The exact relationship between displacements, velocities and acceleration is presented in Appendix J.

The following change of variables is now possible:

$$\mathbf{u}_s = \mathbf{u}_r + \mathbf{I}_{xyz} \mathbf{u}_b, \quad \dot{\mathbf{u}}_s = \dot{\mathbf{u}}_r + \mathbf{I}_{xyz} \dot{\mathbf{u}}_b, \quad \text{and} \quad \ddot{\mathbf{u}}_s = \ddot{\mathbf{u}}_r + \mathbf{I}_{xyz} \ddot{\mathbf{u}}_b \quad (22.5)$$

The matrix  $\mathbf{I}_{xyz} = [\mathbf{I}_x \mathbf{I}_y \mathbf{I}_z]$  and has three columns. The first column has unit values associated with the x displacements, the second column has unit values associated with the y displacements, and the third column has unit values associated with the z displacements. Therefore, the new displacements  $\mathbf{u}_r$  are relative to the specified absolute base displacements. Equation (22.2) can now be rewritten in terms of the relative displacements and the specified base displacements:

$$\mathbf{M}_{ss} \ddot{\mathbf{u}}_r + \mathbf{C}_{ss} \dot{\mathbf{u}}_r + \mathbf{K}_{ss} \mathbf{u}_r = -\mathbf{M}_{ss} \mathbf{I}_{xyz} \ddot{\mathbf{u}}_b - [\mathbf{C}_{ss} \mathbf{I}_{xyz} + \mathbf{C}_{sb}] \dot{\mathbf{u}}_b - [\mathbf{K}_{ss} \mathbf{I}_{xyz} + \mathbf{K}_{sb}] \mathbf{u}_b \quad (22.6)$$

The forces  $[\mathbf{K}_{ss} \mathbf{I}_{xyz} + \mathbf{K}_{sb}] \mathbf{u}_b$  associated with the rigid body displacement of the structure are zero. Because the physical damping matrix is almost impossible to

define, the damping forces on the right-hand side of the equation are normally neglected. Hence, the three-dimensional dynamic equilibrium equations, in terms of relative displacements, are normally written in the following approximate form:

$$\begin{aligned} \mathbf{M}_{ss} \ddot{\mathbf{u}}_r + \mathbf{C}_{ss} \dot{\mathbf{u}}_r + \mathbf{K}_{ss} \mathbf{u}_r &= -\mathbf{M}_{ss} \mathbf{I}_{xyz} \ddot{\mathbf{u}}_b \\ &= -\mathbf{M}_{ss} \mathbf{I}_x \ddot{u}_x(t) - \mathbf{M}_{ss} \mathbf{I}_y \ddot{u}_y(t) - \mathbf{M}_{ss} \mathbf{I}_z \ddot{u}_z(t) \end{aligned} \quad (22.7)$$

Note that the spatial distribution of the loading in the relative formulations is proportional to the directional masses.

{ XE "Higher Mode Damping" } It must be noted that in the absolute displacement formulation, the stiffness matrix  $\mathbf{K}_{sb}$  only has terms associated with the joints adjacent to the base nodes where the displacements are applied. Therefore, the only loads,  $\mathbf{f}_j$ , acting on the structure are point loads acting at a limited number of joints. This type of spatial distribution of point loads excites the high frequency modes of the system as the displacements are propagated within the structure. Hence, the physical behavior of the analysis model is very different if displacements are applied rather than if the mass times the acceleration is used as the loading. Therefore, the computer program user must understand that both approaches are approximate for non-zero damping.

If the complete damping matrix is specified and the damping terms on the right-hand sides of Equations (22.2 and 22.6) are included, an exact solution of both the absolute and relative formulations will produce identical solutions.

### 22.3 USE OF PSEUDO-STATIC DISPLACEMENTS

An alternate formulations, which is restricted to linear problems, is possible for multi support displacement loading that involves the use of pseudo-static displacements, which are defined as:

$$\mathbf{u}_p = -\mathbf{K}_{ss}^{-1} \mathbf{K}_{sb} \mathbf{u}_b = \mathbf{T} \mathbf{u}_b \quad (22.8)$$

The following change of variable is now introduced:

$$\mathbf{u}_s = \mathbf{u} + \mathbf{u}_p = \mathbf{u} + \mathbf{T}\mathbf{u}_b, \quad \dot{\mathbf{u}}_s = \dot{\mathbf{u}} + \mathbf{T}\dot{\mathbf{u}}_b \text{ and } \ddot{\mathbf{u}}_s = \ddot{\mathbf{u}} + \mathbf{T}\ddot{\mathbf{u}}_b \quad (22.9)$$

The substitution of Equations (9) into Equation (2) yields the following set of equilibrium equations:

$$\begin{aligned} \mathbf{M}_{ss}\ddot{\mathbf{u}} + \mathbf{C}_{ss}\dot{\mathbf{u}} + \mathbf{K}_{ss}\mathbf{u} = & -\mathbf{K}_{sb}\mathbf{u}_b - \mathbf{C}_{sb}\dot{\mathbf{u}}_b - \mathbf{M}_{ss}\mathbf{T}\ddot{\mathbf{u}}_b \\ & - \mathbf{C}_{ss}\mathbf{T}\dot{\mathbf{u}}_b - \mathbf{K}_{ss}\mathbf{T}\mathbf{u}_b \end{aligned} \quad (22.10)$$

Hence Equation (22.10) can be written in the following simplified form:

$$\mathbf{M}_{ss}\ddot{\mathbf{u}} + \mathbf{C}_{ss}\dot{\mathbf{u}} + \mathbf{K}_{ss}\mathbf{u} = -\mathbf{M}_{ss}\mathbf{T}\ddot{\mathbf{u}}_b - [\mathbf{C}_{sb} + \mathbf{C}_{ss}\mathbf{T}]\dot{\mathbf{u}}_b \quad (22.11)$$

Equation (22.11) is exact if the damping terms are included on the right-hand side of the equation. However, these damping terms are normally not defined and are neglected. Hence, different results will be obtained from this formulation when compared to the absolute displacement formulation. The pseudo-static displacements cannot be extended to nonlinear problems; therefore, it cannot be considered a general method that can be used for all structural systems.

## 22.4 SOLUTION OF DYNAMIC EQUILIBRIUM EQUATIONS

The absolute displacement formulation, Equation (22.3), and the relative formulation, Equation (22.7), can be written in the following generic form:

$$\mathbf{M}\ddot{\mathbf{u}}(t) + \mathbf{C}\dot{\mathbf{u}}(t) + \mathbf{K}\mathbf{u}(t) = \sum_{j=1}^J \mathbf{f}_j g_j(t) \quad (22.12)$$

Many different methods can be used to solve the dynamic equilibrium equations formulated in terms of absolute or relative displacements. The direct incremental numerical integration can be used to solve these equations. However, because of stability problems, large damping is often introduced in the higher modes, and only an approximate solution that is a function of the size of the time step used is obtained. The frequency domain solution using the **Fast-Fourier-Transform**, FFT, method also produces an approximate solution. Therefore, the errors identified in this paper exist for all methods of dynamic response analysis. Only the mode superposition method, for both linear acceleration and cubic

displacement loads, can be used to produce an exact solution. This approach is presented in Chapter 13.

## 22.5 NUMERICAL EXAMPLE

### 22.5.1 Example Structure

The problems associated with the use of absolute displacement as direct input to a dynamic analysis problem can be illustrated by the numerical example shown in Figure 22.2.

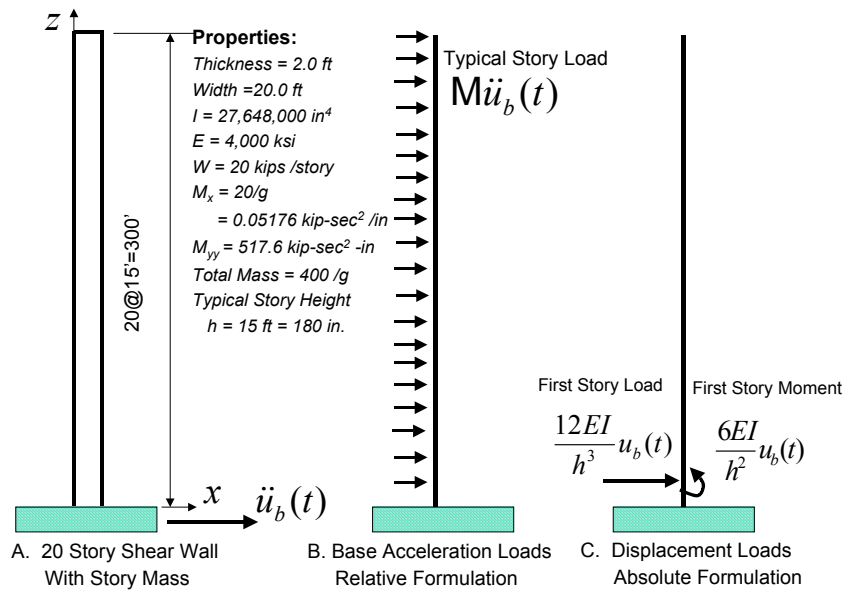


**Figure 22.2 Comparison of Relative and Absolute Displacement Seismic Analysis**

Neglecting shear and axial deformations, the model of the structure has forty displacement degrees of freedom, one translation and one rotation at each joint. The rotational masses at the nodes have been included; therefore, forty modes of vibration exist. Note that loads associated with the specification of the absolute base displacements are concentrated forces at the joint near the base of the structure. The exact periods of vibration for these simple cantilever structures are summarized in Table 22.1 in addition to the mass, static and dynamic load-

participation factors. The derivations of mass-participation factor, static-participation factors, and dynamic-participation factors are given in Chapter 13.

**Table 22.1 Periods and Participation Factors for Exact Eigenvectors**

Mode Number	Period (Seconds)	Cumulative Sum of Mass Participation Factors X-Direction (Percentage)	Cumulative Sum of Load Participation Factors Base Displacement Loading (Percentage)	
			Static	Dynamic
1	1.242178	62.645	0.007	0.000
2	0.199956	81.823	0.093	0.000
3	0.072474	88.312	0.315	0.000
4	0.037783	91.565	0.725	0.002
5	0.023480	93.484	1.350	0.007
6	0.016227	94.730	2.200	0.023
7	0.012045	95.592	3.267	0.060
8	0.009414	96.215	4.529	0.130
9	0.007652	96.679	5.952	0.251
10	0.006414	97.032	7.492	0.437
11	0.005513	97.304	9.099	0.699
12	0.004838	97.515	10.718	1.042
13	0.004324	97.678	12.290	1.459
14	0.003925	97.804	13.753	1.930
15	0.003615	97.898	15.046	2.421
16	0.003374	97.966	16.114	2.886
17	0.003189	98.011	16.913	3.276
18	0.003052	98.038	17.429	3.551
19	0.002958	98.050	17.683	3.695
20	0.002902	98.053	17.752	3.736
21	0.002066	99.988	99.181	98.387
30	0.001538	99.999	99.922	99.832
40	0.001493	100.000	100.000	100.000



It is important to note that only four modes are required to capture over 90 percent of the mass in the x-direction. However, for displacement loading, 21 eigenvectors are required to capture the static response of the structure and the kinetic energy under rigid-body motion. Note that the period of the 21<sup>th</sup> mode is 0.002066 seconds, or approximately 50 cycles per second. However, this high frequency response is essential so that the absolute base displacement is accurately propagated into the structure.

### 22.5.2 Earthquake Loading

The acceleration, velocity and displacement base motions associated with an idealized near-field earthquake are shown in Figure 22.3. The motions have been selected to be simple and realistic so that this problem can be easily solved using different dynamic analysis programs.

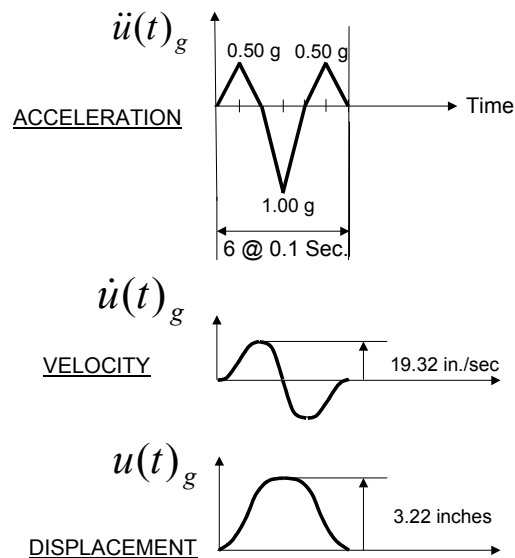


*Figure 22.3 Idealized Near-Field Earthquake Motions*

### 22.5.3 Effect of Time Step Size for Zero Damping

{ XE "Time Step Size" }To illustrate the significant differences between acceleration and displacement loading, this problem will be solved using all forty eigenvectors, zero damping and three different integration time steps. The

absolute top displacement, base shears and moments at the second level are summarized in Table 22.2. In addition, the maximum input energy and kinetic energy in the model are summarized.

**Table 22.2 Comparison of Acceleration and Displacement Loads (40 Eigenvalues – 0.0 Damping Ratio)**

	Linear Acceleration Loads			Linear Displacement Loads		
	$\Delta t = 0.01$	$\Delta t = 0.005$	$\Delta t = 0.001$	$\Delta t = 0.01$	$\Delta t = 0.005$	$\Delta t = 0.001$
$u_{20}$ (Inches)	5.306 @ 0.610	5.306 @0.610	5.306 @0.610	5.306 @0.610	5.307 @0.610	5.307 @0.610
$V_2$ (Kips)	-94.35 @0.310	-94.35 @0.310	-94.58 @0.308	-90.83 @0.660	-74.74 @0.310	94.91 @0.308
$M_2$ (K - In.)	-149,500 @0.610	-149,500 @0.610	-149,500 @0.610	-152,000 @0.610	-148,100 @0.605	-149,500 @0.610
ENERGY (Input To Model)	339.9 @0.410	339.9 @0.405	340.0 @0.401	1,212,000 @0.310	1,183,000 @0.305	1,180,000 @0.301
K-ENERGY (Within Model)	339.9 @0.410	339.9 @0.405	339.9 @0.402	166.2 @0.410	164.1 @0.405	163.9 @0.402

For linear acceleration load, all results are exact regardless of the size of the time step because the integration algorithm is based on the exact solution for a linear function. The minor difference in results is because some maximum values occur within the larger time step results. However, using the same linear integration algorithm for displacement loads produces errors because displacements are cubic function within each time step (Appendix J). Therefore, the larger the time step, the larger the error.

For linear displacement loads, the maximum displacement at the top of the structure and the moment  $t$  at the second level appear to be insensitive to the size of the time step. However, the forces near the top of the structure and the shear at the second level can have significant errors because of large integration time steps. For a time step of 0.01 seconds, the maximum shear of -90.83 kips occurs at 0.660 seconds; whereas, the exact value for the same time step is -94.35 kips

and occurs at 0.310 seconds. A time-history plot of both shears forces is shown in Figure 22.4.

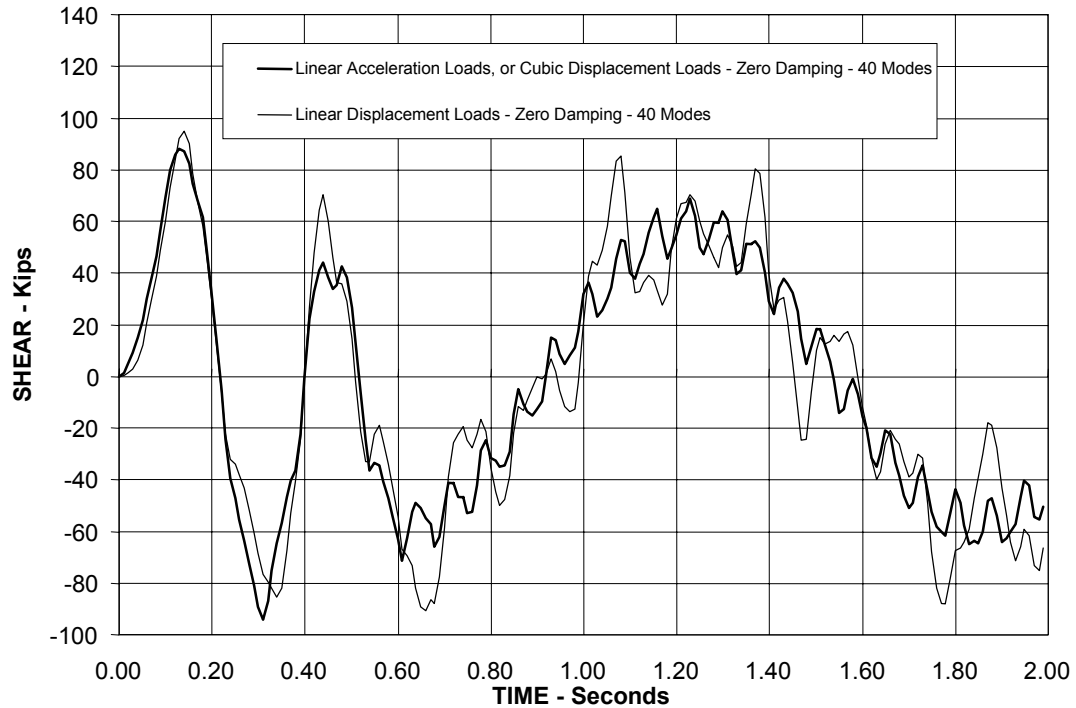


*Figure 22.4 Shear at Second Level Vs. Time With  $\Delta t = 0.01$ -Seconds and Zero Damping*

The errors resulting from the use of large time steps are not large in this example because the loading is a simple function that does not contain high frequencies. However, the author has had experience with other structures, using real earthquake displacement loading, where the errors are over 100 percent using a time step of 0.01 seconds. The errors associated with the use of large time steps in a mode superposition analysis can be eliminated for linear elastic structures using the new exact integration algorithm presented in Chapter 13.

An examination of the input and kinetic energy clearly indicates that there is a major *mathematical* differences between acceleration loads (relative displacement formulation) and displacement loads (absolute displacement formulation). In the relative displacement formulation, a relatively small amount

of energy, 340 k-in, is supplied to the mathematical model; whereas the point loads associated with the absolute formulation applied near the base of the structure imparts over 1,000,000 k-in of energy to the model. Also, the maximum kinetic energy (proportional to the sum of mass times velocity squared) within the model is 340 k-in for the relative formulation compared to 164 kip-in for the absolute formulation.

The results clearly indicate that errors are introduced if large time steps are used with the linear displacement approximation within each time step. The spatial load distribution is significantly different between the relative and displacement formulations. For linear acceleration loads, large time steps can be used. However, very small time steps, 0.001 second, are required for absolute displacement loading to obtain accurate results. However, if modal superposition is used, the new cubic displacement load approximation produces results identical to those obtained using linear acceleration loads for zero damping.

#### **22.5.4 Earthquake Analysis with Finite Damping**

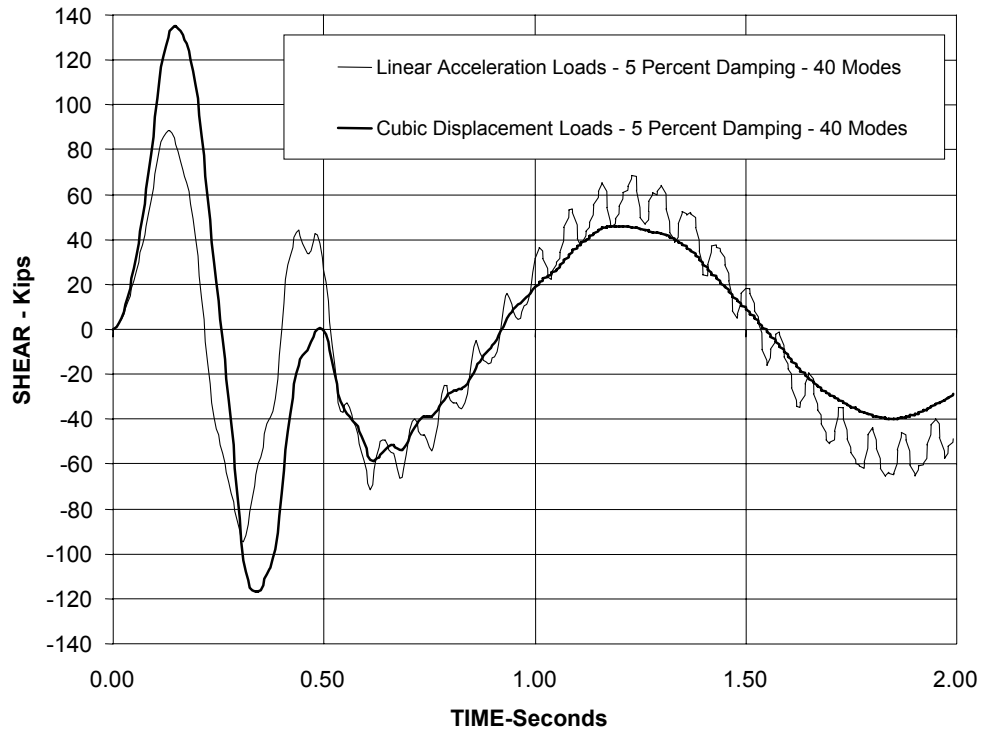
It is very important to understand that the results produced from a mathematical computer model may be significantly different from the behavior of the real physical structure. The behavior of a real structure will satisfy the basic laws of physics, whereas the computer model will satisfy the laws of mathematics after certain assumption have been made. The introduction of classical linear viscous damping will illustrate this problem.

Table 22.3 summarizes selective results of an analysis of the structure shown in Figure 22.2 for both zero and five percent damping for all frequencies. The time step used for this study is 0.005 second; hence, for linear acceleration loads and cubic displacement loads, exact results (within three significant figures) are produced.

The results clearly indicate that 5 percent damping produces different results for acceleration and displacement loading. The top displacements and the moments near the base are very close. However, the shear at the second level and the moment at the tenth level are significantly different. The shears at the second level vs. time for displacement loading are plotted in Figure 22.5 for 5 percent damping.

**Table 22.3. Comparison of Acceleration and Displacement Loads for Different Damping (40 Eigenvalues, 0.005 Second Time Step)**

	Linear Acceleration Loads		Cubic Displacement Loads	
	$\xi = 0.00$	$\xi = 0.05$	$\xi = 0.00$	$\xi = 0.05$
$u_{20}$ (Inch)	5.306 @ 0.610 -5.305 @ 1.230	4.939 @ 0.580 -4.217 @ 1.205	5.307 @ 0.610 -5.304 @ 1.230	4.913 @ 0.600 -4.198 @ 1.230
$V_2$ (Kips)	88.31 @ 0.130 -94.35 @ 0.310	84.30 @ 0.130 -95.78 @ 0.310	88.28 @ 0.135 -94.53 @ 0.310	135.1 @ 0.150 -117.1 @ 0.340
$M_2$ (K-in.)	148,900 @ 1.230 -149,500 @ 0.605	116,100 @ 1.200 -136,300 @ 0.610	148,900 @ 1.230 -149,500 @ 0.605	115,300 @ 1.230 -136,700 @ 0.605
$M_{10}$ (K-in.)	81,720 @ 0.290 -63,470 @ 0.495	77,530 @ 0.300 -64,790 @ 0.485	81,720 @ 0.290 -63,470 @ 0.495	80,480 @ 0.320 -59,840 @ 0.495



**Figure 22.5 Shear at Second Level Vs. Time Due To Cubic Displacement Loading. (40 Eigenvalues –  $\Delta t = 0.005$  Seconds)**

The results shown in Figure 22.5 are physically impossible for a real structure because the addition of 5 percent damping to an undamped structure should not increase the maximum shear from 88.28 kips to 135.10 kips. The reason for this violation of the fundamental laws of physics is the invalid assumption of an orthogonal damping matrix required to produce *classical damping*.

Classical damping always has a mass-proportional damping component, as physically illustrated in Figure 22.6, which causes external velocity-dependent forces to act on the structure. For the relative displacement formulation, the forces are proportional to the relative velocities. Whereas for the case of the application of base displacement, the external force is proportional to the absolute velocity. Hence, for a rigid structure, large external damping forces can be developed because of rigid body displacements at the base of the structure. This is the reason that the shear forces increase as the damping is increased, as shown in Figure 22.6. For the case of a very flexible (or base isolated) structure, the relative displacement formulation will produce large errors in the shear forces because the external forces at a level will be carried direct by the dash-pot at that level. Therefore, neither formulation is physically correct.

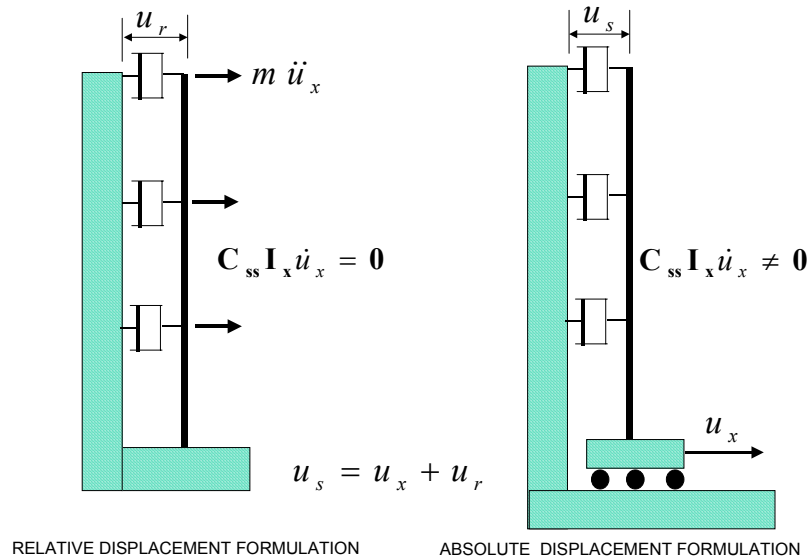


**Figure 22.6 Example to Illustrate Mass-Proportional Component in Classical Damping.**

These inconsistent damping assumptions are inherent in *all methods* of linear and nonlinear dynamic analysis that use classical damping or mass-proportional damping. For most applications, this damping-induced error may be small; however, the engineer/analyst has the responsibility to evaluate, using simple linear models, the magnitude of those errors for each different structure and earthquake loading.

### 22.5.5 The Effect of Mode Truncation

{ XE "Mode Truncation" }The most important difference between the use of relative and absolute displacement formulations is that higher frequencies are excited by base displacement loading. Solving the same structure using a different number of modes can identify this error. If zero damping is used, the equations of motions can be evaluated exactly for both relative and absolute displacement formulations and the errors associated with mode-truncation only can be isolated.

Selective displacements and member forces for both formulations are summarized in Table 22.4.

**Table 22.4 Mode-Truncation Results - Exact Integration for 0.005 Second Time Steps – Zero Damping**

Number of Modes	Linear Acceleration Loads				Cubic Displacement Loads			
	$u_{20}$	$V_2$	$M_2$	$M_{10}$	$u_{20}$	$V_2$	$M_2$	$M_{10}$
4	5.306	83.10	-149,400	81,320	5.307	-51,580	-1,441,000	346,800
10	5.306	-94.58	-149,500	81,760	5.307	-33,510	-286,100	642,100
21	5.306	-94.73	-149,500	81,720	5.307	-55,180	-4,576,000	78,840
30	5.306	-94.42	149,500	81,720	5.307	-11,060	-967,200	182,400
35	5.306	94.35	149,500	81,720	5.307	-71,320	-149,500	106,100
40	5.306	-94.35	-149,500	81,720	5.307	-94.53	-149,500	81,720

The results shown in Table 22.4 clearly indicate that only a few modes are required to obtain a converged solution using the relative displacement formulation. However, the results using the absolute displacement formulation are almost unbelievable. The reason for this is that the computational model and

the real structure are required to propagate the high frequencies excited by the base displacement loading into the structure. The displacement at the top of the structure, which is dominated by the first mode, is insensitive to the high frequency wave propagation effects. However, the shear and moment forces within the structure will have significant errors if all the frequencies are not present in the analysis. Table 22.5 summarizes selective displacements and member forces for both formulations for 5 percent damping.

**Table 22.5 Mode-Truncation Errors - Exact Integration for 0.005 Second Time Steps – 5 % Damping**

Number of Modes	Linear Acceleration Loads				Cubic Displacement Loads			
	$u_{20}$	$V_2$	$M_2$	$M_{10}$	$u_{20}$	$V_2$	$M_2$	$M_{10}$
4	4.934	-82.51	-136,300	77,110	4.913	-5,153	1,439,000	374,600
10	4.939	-96.01	-136,300	-64,810	4.913	-33,500	-290,000	640,900
21	4.939	-96.16	-136,300	-64,790	4.913	-55,170	-4,573,000	77,650
30	"	"	"	"	4.913	-11,050	-966,000	180,800
35	"	"	"	"	4.913	-342.7	-136,800	104,500
40	"	"	"	"	4.913	-135.1	-136,800	80,480

The results shown in Table 22.5 indicate that the addition of modal damping does not significantly change the fundamental behavior of the computational model. It is apparent that a large number of high frequencies must be included in the analysis if the computational model is to accurately predict forces in the real structure. It is of considerable interest, however, that mode truncation for this problem produces erroneously large forces that are difficult to interpret. To explain those errors, it is necessary to examine the individual mode shapes. For example, the 21st mode is a lateral displacement at the second level only, with all other mode displacement near zero. This is a very important mode because a concentrated force associated with the base displacement loading is applied at the second level. Hence, the addition of that mode to the analysis increases the bending moment at the second level to 4,573,000 and decreases the moment at the 10<sup>th</sup> level to 77,650. Additional modes are then required to reduce the internal forces at the second level.



## 22.6 USE OF LOAD DEPENDENT RITZ VECTORS

In Table 22.6 the results of an analysis using different numbers of Load Dependent Ritz vectors is summarized. In addition, mass, static and dynamic participation factors are presented.

**Table 22.6 Results Using LDR Vectors- $\Delta t = 0.005$  Cubic Displacement Loading – Damping = 5 %**

Number of Vectors	$u_{20}$	$V_2$	$M_2$	$M_{10}$	Mass, Static and Dynamic Load-Participation
4	4.913	111.4	-136,100	80,200	100. 100. 29.5
7	4.913	132.6	-136,700	80,480	100. 100. 75.9
10	4.913	134.5	-136,800	80,490	100. 100. 98.0
21	4.913	135.1	-136,800	80,480	100. 100. 100.
30	4.913	135.1	-136,800	80,480	100. 100. 100.

The use of LDR vectors virtually eliminates all problem associated with the use of the exact eigenvectors. The reason for this improved accuracy is that each set of LDR vectors contains the static response of the system. To illustrate this, the fundamental properties of a set of seven LDR vectors are summarized in Table 22.7.

**Table 22.7 Periods and Participation Factors for LDR Vectors**

Vector Number	Approximate Period (Seconds)	Cumulative Sum of Mass Participation Factors X-Direction (Percentage)	Cumulative Sum of Load Participation Factors Base Displacement Loading (Percentage)	
			Static	Dynamic
1	1.242178	62.645	0.007	0.000
2	0.199956	81.823	0.093	0.000
3	0.072474	88.312	0.315	0.000
4	0.037780	91.568	0.725	0.002
5	0.023067	93.779	1.471	0.009
6	0.012211	96.701	5.001	0.126
7	0.002494	100.000	100.00	75.882

The first six LDR vectors are almost identical to the exact eigenvectors summarized in Table 22.1. However, the seventh vector, which is a linear combination of the remaining eigenvectors, contains the high frequency response of the system. The period associated with this vector is over 400 cycles per second; however, it is the most important vector in the analysis of a structure subjected to base displacement loading.

## 22.7 SOLUTION USING STEP-BY-STEP INTEGRATION

{ XE "Step By Step Integration" } The same problem is solved using direct integration by the trapezoidal rule, which has no numerical damping and theoretically conserves energy. However, to solve the structure with zero damping, a very small time step would be required. It is almost impossible to specify constant modal damping using direct integration methods. A standard method to add energy dissipation to a direct integration method is to add Rayleigh damping, in which only damping ratios can be specified at two frequencies. For this example 5 percent damping can be specified for the lowest frequency and at 30 cycles per second. Selective results are summarized in Table 22.8 for both acceleration and displacement loading.

**Table 22.8 Comparison of Results Using Constant Modal Damping and the Trapezoidal Rule and Rayleigh Damping (0.005 Second Time Step)**

	Acceleration Loading		Displacement Loading	
	Trapezoidal Rule Using Rayleigh Damping	Exact Solution Using Constant, Modal Damping $\xi = 0.05$	Trapezoidal Rule Using Rayleigh Damping	Exact Solution Using Constant, Modal Damping $\xi = 0.05$
$u_{20}$ (Inch)	4.924 @ 0.580 -4.217 @ 1.200	4.939 @ 0.580 -4.217 @ 1.205	4.912 @ 0.600 -4.182 @ 1.220	4.913 @ 0.600 -4.198 @ 1.230
$V_2$ (Kips)	86.61 @ 0.125 -95.953 @ 0.305	84.30 @ 0.130 -95.78 @ 0.310	89.3 @ 0.130 -93.9 @ 0.305	135.1 @ 0.150 -117.1 @ 0.340
$M_2$ (k-in.)	115,600 @ 1.185 -136,400 @ 0.605	116,100 @ 1.200 -136,300 @ 0.610	107,300 @ 1.225 -126,300 @ 0.610	115,300 @ 1.230 -136,700 @ 0.605
$M_{10}$ (K-in.)	78,700 @ 0.285 -64,500 @ 0.485	77,530 @ 0.300 -64,790 @ 0.485	81,300 @ 0.280 61,210 @ 0.480	80,480 @ 0.320 -59,840 @ 0.495

It is apparent that the use of Rayleigh damping for acceleration loading produces a very good approximation of the exact solution using constant modal damping. However, for displacement loading, the use of Rayleigh damping, in which the high frequencies are highly damped and some lower frequencies are under damped, produces larger errors. A plot of the shears at the second level using the different methods is shown in Figure 22.7. It is not clear if the errors are caused by the Rayleigh damping approximation or by the use of a large time step.

It is apparent that errors associated with the unrealistic damping of the high frequencies excited by displacement loading are present in all step-by-step integration methods. It is a property of the mathematical model and is not associated with the method of solution of the equilibrium equations.

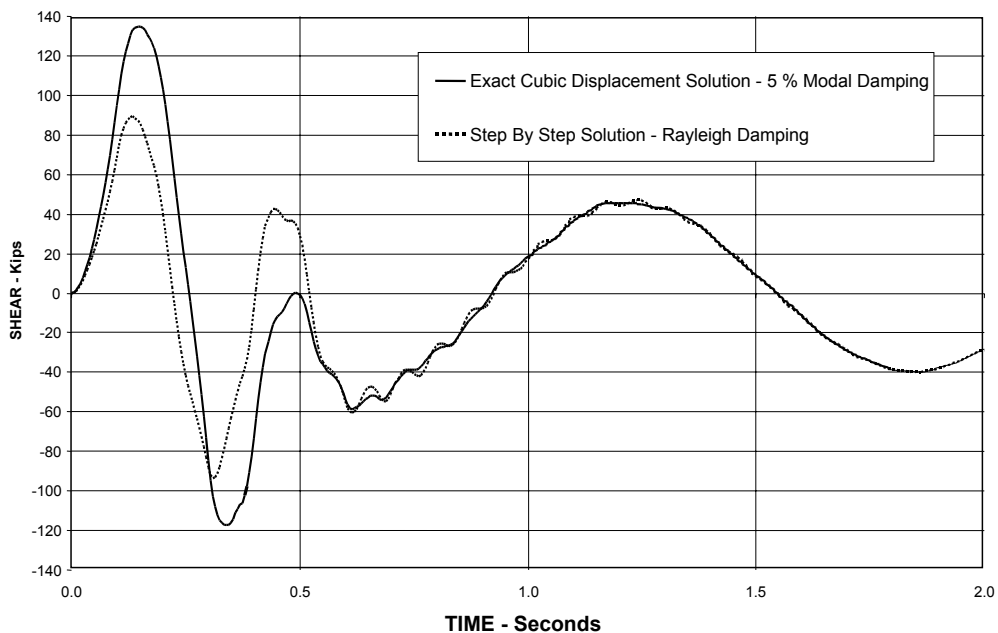


**Figure 22.7 Comparison of Step-By-Step Solution Using the Trapezoidal Rule and Rayleigh Damping with Exact Solution (0.005 second time-step and 5% damping)**

The effective damping in the high frequencies, using displacement loading and Rayleigh damping, can be so large that the use of large numerical integration time steps produces almost the same results as using small time steps. However,

the accuracy of the results cannot be justified using this argument, because the form of the Rayleigh damping used in the computer model is physically impossible within a real structure. In addition, the use of a numerical integration method that produces numerical energy dissipation in the higher modes may produce unrealistic result when compared to an exact solution using displacement loading.

## 22.8 SUMMARY

Several new sources of numerical errors associated with the direct application of earthquake displacement loading have been identified. Those problems are summarized as follows:

1. Displacement loading is fundamentally different from acceleration loading because a larger number of modes are excited. Hence, a very small time step is required to define the displacement record and to integrate the dynamic equilibrium equations. A large time step, such as 0.01 second, can cause significant unpredictable errors.
2. The effective damping associated with displacement loading is larger than that for acceleration loading. The use of mass proportional damping, inherent in Rayleigh and classical modal damping, cannot be physically justified.
3. Small errors in maximum displacements do not guarantee small errors in member forces.
4. The 90 percent mass participation rule, which is used to estimate errors for acceleration loading, does not apply to displacement loading. A larger number of modes are required to accurately predict member forces for absolute displacement loading.
5. For displacement loading, mode truncation in the mode superposition method may cause large errors in the internal member forces.

The following numerical methods can be used to minimize those errors:

1. A new integration algorithm based on cubic displacements within each time step allows the use of larger time steps.
2. To obtain accurate results, the static load-participation factors must be very close to 100 percent.
3. The use of LDR vectors will significantly reduce the number of vectors required to produce accurate results for displacement loading.
4. The example problem illustrates that the errors can be significant if displacement loading is applied based on the same rules used for acceleration loading. However, additional studies on different types of structures, such as bridge towers, must be conducted. Also, more research is required to eliminate or justify the differences in results produced by the relative and absolute displacement formulations for non-zero modal damping.

Finally, the state-of-the-art use of classical modal damping and Rayleigh damping contains mass proportional damping that is physically impossible. Therefore, the development of a new mathematical energy dissipation model is required if modern computer programs are to be used to accurately simulate the true dynamic behavior of real structures subjected to displacement loading.

— |

| —

22-22

STATIC AND DYNAMIC ANALYSIS

— |

| —